Green Chemistry

PAPER

View Article Online
View Journal | View Issue

Cite this: *Green Chem.*, 2022, **24**, 5320

Electrosynthesis of amino acids from biomass-derived α-hydroxyl acids†

Kaili Yan, Morgan L. Huddleston, Brett A. Gerdes and Yujie Sun *

Received 11th May 2022,
Accepted 4th June 2022

DOI: 10.1039/d2gc01779b

rsc.li/greenchem

Electrochemical conversion of biomass-derived intermediate compounds to high-value products has emerged as a promising approach in the field of biorefinery. Biomass upgrading allows for the production of chemicals from non-fossil-based carbon sources and capitalization on electricity as a green energy input. Amino acids, as products of biomass upgrading, have received relatively little attention. Pharmaceutical and food industries will benefit from an alternative strategy for the production of amino acids that does not rely on inefficient fermentation processes. The use of renewable biomass resources as starting materials makes this proposed strategy more desirable. Herein, we report an electrochemical approach for the selective oxidation of biomass-derived α-hydroxyl acids to α-keto acids, followed by electrochemical reductive amination to yield amino acids as the final products. Such a strategy takes advantage of both reactions at the anode and cathode and produces amino acids under ambient conditions with high energy efficiency. A flow electrolyzer was also successfully employed for the conversion of α-hydroxyl acids to amino acids, highlighting its great potential for large-scale application.

Introduction

Due to the depletion of fossil reserves, increasing interest has been devoted to fundamentally shifting the chemical industry from fossil fuels to sustainable carbon sources. Biomass is the only renewable carbon source whose utilization will not alter our current ecosystem and is globally accessible with a large scale. Recent years have witnessed the emergence of novel biomass upgrading strategies,[1,2] among which electrochemical conversion is particularly appealing because the utilized electricity can be derived from sustainable energy resources, such as solar and wind. Hence, many research groups have been developing a variety of electrocatalytic systems for biomass valorization, with a particular focus on generating high-value products.[3–7]

Despite increasing efforts in targeting a large number of value-added products from biomass upgrading, the electrochemical production of amino acids from biomass-derived α-hydroxyl acids has received little attention. In fact, amino acids are essential building blocks of proteins[8] and therefore play an important role in various industrial sectors ranging from food and agriculture to pharmaceuticals.[9–11] Nevertheless, not many economically attractive chemical approaches have been developed for the production of amino acids on a large scale yet. The earliest example of this process is the Strecker synthesis, which is applied to methionine production on an industrial scale.[12,13] However, one of the apparent disadvantages of this method is the requirement of using highly toxic cyanides as the nitrogen source (Fig. 1a). Currently, amino acids are primarily produced from microbial conversion processes.[14,15] However, these biological-based processes bear many drawbacks, such as slow production rate and high energy usage. Furthermore, the challenging separation of amino acids from bio-based intermediates, acids, and liquid media inevitably escalates the overall cost of the fermentation process and simultaneously results in a large amount of waste salts. Consequently, an alternative greener strategy for the large-scale production of amino acids from sustainable carbon source is highly desirable.

Indeed, novel catalytic strategies have been reported recently to explore the production of amino acids from biomass-derived molecules. For instance, carbon nanotubes decorated with ruthenium nanoparticles were reported to catalyze the synthesis of amino acids from lignocellulose-derived α-hydroxyl acids (Fig. 1a).[16] However, this strategy requires noble metal catalysts, high temperature, and elevated pressure of H_2. Ultrathin CdS nanosheets were recently reported as a competent photocatalyst in converting α-hydroxyl acids into bio-amino acids under visible light irradiation (Fig. 1a).[17] Unfortunately, the overall yields of amino acids are limited (<30%) and several acid substrates, such as 3-hydroxypropionic acid or mandelic acid, exhibited no conversion. Compared to all the reported processes, electrosynthesis has been regarded

Department of Chemistry, University of Cincinnati, Cincinnati, OH 45221, USA. E-mail: yujie.sun@uc.edu

† Electronic supplementary information (ESI) available. See DOI: https://doi.org/10.1039/d2gc01779b

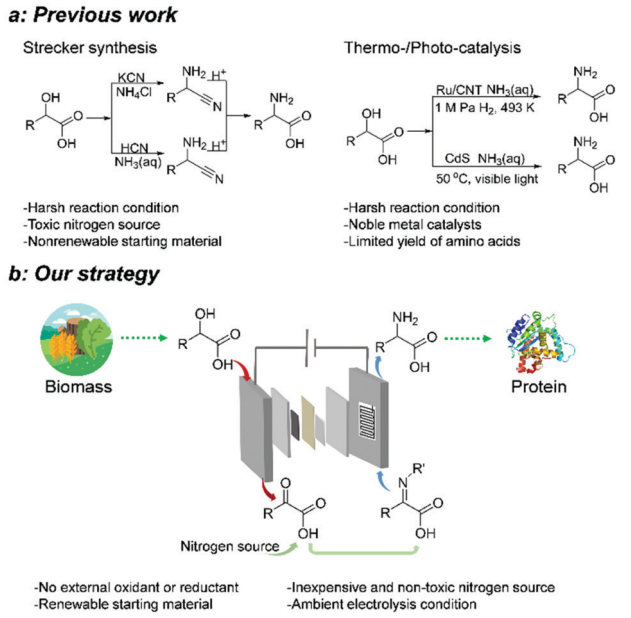

Fig. 1 (a) Reported Strecker and thermocatalytic/photocatalytic strategies for the synthesis of amino acids. (b) Our electrochemical approach for the production of amino acids from biomass-derived α-hydroxyl acids in a flow cell.

as a sustainable and efficient method, as it does not require any external oxidants/reductants and is usually carried out under ambient conditions.[18–20]

Indeed, electrochemical reductive amination has been reported for the synthesis of amino acids from α-keto acids in a flow electrolyzer when NH_2OH was employed as the nitrogen source.[21] In this case, the counter reaction is water oxidation and IrO_2 was used as the anode to drive the oxygen evolution reaction (OER). Since α-keto acids are downstream products of α-hydroxyl acids, which are readily available from lignocellulosic biomass and regarded as more attractive feedstocks for amino acids synthesis,[22–24] we reasoned that it would be more economically appealing to electrochemically synthesize amino acids from biomass-derived α-hydroxyl acids. Such a strategy will completely avoid the energetically demanding and kinetically slow OER, which produces O_2 of little value. Instead, thermodynamically more favourable α-hydroxyl acid oxidation to α-keto acids will take place at the anode, substantially increasing the energy efficiency of an electrolyzer. Herein, we report an electrochemical approach that couple the oxidation of α-hydroxyl acids to α-keto acids at the anode with the reductive amination of α-keto acids to amino acids at the cathode. Consequently, higher reaction rates and yields of amino acids are achievable compared to those of the aforementioned electrochemical strategy. It should be noted that our strategy takes advantage of both anode and cathode reactions to minimize energy input. This approach allows for the direct utilization of biomass-derived α-hydroxyl acids to generate amino acids with high yields. Electrolysis using a flow electrolyzer was also successfully demonstrated, highlighting the potential for large-scale production.[25–27] Compared to all of the previous methods discussed above, our strategy demonstrates apparent economic advantages.

As schematically displayed in Fig. 1b, our electrochemical strategy starts from the selective oxidation of biomass-derived α-hydroxyl acids to produce α-keto acids in the anodic chamber of a flow cell. The newly generated α-keto acids will react with a nitrogen source (NH_3 or NH_2OH) to form an imine or oxime intermediate under ambient conditions, which can be directly subjected to electrochemical hydrogenation in the cathodic chamber of the same flow cell. Such an electrochemical process requires no external oxidant or reductant, but only inexpensive reagents and biomass-derived starting materials. Additionally, this reaction can be performed under mild conditions (*e.g.*, room temperature and atmospheric pressure).

Experimental

All chemicals were purchased from commercial vendors and used as received. Lithium perchlorate, hydroxylammonium chloride, 1,3,5-trimethoxybenzene, maleic acid, *N*-hydroxyphthalimide, 2,6-lutidine, (2,2,6,6-tetramethylpiperidin-1-yl)oxyl, and ammonium solution (25%) were purchased from Sigma-Aldrich. DL-Mandelic acid, phenylglyoxylic acid, 2-phenylglycine, DL-3-phenyllactic acid, phenylpyruvic acid, phenylalanine, glycolic acid, glyoxylic acid, glycine, lactic acid, pyruvic acid, DL-alanine, 2-hydroxy-4-methylpentanoic acid, 4-methyl-2-oxovaleric acid, and leucine were purchased from Ambeed, Inc. Ti foil, carbon paper, and anion exchange membrane (Fumasep FAB-PK-130) were purchased from Fuel Cell Store.

Electrochemical measurements were performed using a Biologic VSP potentiostat. For the selective oxidation of α-hydroxyl acids, *N*-hydroxyphthalimide (NHPI) or (2,2,6,6-tetramethylpiperidin-1-yl)oxyl (TEMPO) was used as the redox mediator and 2,6-lutidine as the Lewis base. Carbon paper was used as the working electrode, Ag/Ag^+ electrode was used as the reference electrode, and a Pt wire was used as the counter electrode, with 0.1 M $LiClO_4$ MeCN/H_2O (v/v: 2/1) as the electrolyte. For the electroreductive amination of α-keto acids, Ti foil was used as the working electrode, a Ag/Ag^+ electrode as the reference electrode, and a Pt wire as the counter electrode with 0.1 M $LiClO_4$ MeCN/H_2O (v/v: 2/1) as electrolyte in a H-cell. Cathode electrolyte was formed by stirring 20 mM α-keto acids with 1.2–1.5 equivalents of NH_3 (aq.) or $NH_2OH{\cdot}HCl$ in 0.1 M $LiClO_4$ MeCN/H_2O (v/v: 2/1) overnight at room temperature prior to electrochemical experiments.

Eight pieces of carbon paper (1×1 cm^2) and eight pieces of Ti foil (1×1 cm^2) were compressed and used as the working and counter electrodes, respectively, for flow electrolysis. The working and counter chambers were separated by an organic anion exchange membrane (Fumasep FAB-PK-130). Corresponding electrolytes described above were used in a similar fashion for flow electrolysis with a flow rate of 0.8 mL min^{-1}. For the quantification of phenylglyoxylic acid and phe-

nylpyruvic acid, 20 μL of the electrolyte solution in the anode chamber was collected periodically during electrolysis and diluted with 1 mL MeOH and then analyzed by HPLC equipped with a C18 column using an eluent solvent mixture of 5 mM ammonium acetate/acetonitrile (v/v = 95/5). Proton NMR was used to quantify 4-methyl-2-oxovaleric acid, glyoxylic acid, pyruvic acid, glycine (Gly), alanine (Ala), and leucine (Leu) using maleic acid as the internal standard, while 1,3,5-trimethoxybenzene was employed as the internal standard to quantify 2-phenylglycine and phenylalanine (Phe).

Results and discussion

Our research endeavour started from the selective oxidation of α-hydroxyl acids to keto acids utilizing appropriate redox mediators. Electrochemical oxidation of alcohols using inexpensive electrocatalysts has been well reported,[28–31] which most commonly results in carboxylic acids as the final products. In contrast, finely controlled selective oxidation of an alcohol group to an aldehyde or a ketone group is more challenging, especially in the presence of an adjacent carboxylic acid group. In order to realize our designed strategy, the first critical step is the electrochemical oxidation of α-hydroxyl acids to keto acids without the loss of the carboxylic acid groups. Since *N*-hydroxyphthalimide (NHPI) has been successfully utilized for the partial oxidation of primary and secondary alcohols to yield aldehydes and ketones,[32–35] we decided to conduct our desirable oxidation using NHPI as the redox mediator and DL-mandelic acid as the first α-hydroxyl acid substrate. It should be noted that DL-mandelic acid is a readily available feedstock from glucose.[36] As shown in Fig. 2a, the partial oxidation of the alcohol group in DL-mandelic acid will produce phenylglyoxylic acid as the desired product, while further oxidative cleavage of the carboxylic group will yield benzoic acid, an undesirable side product.

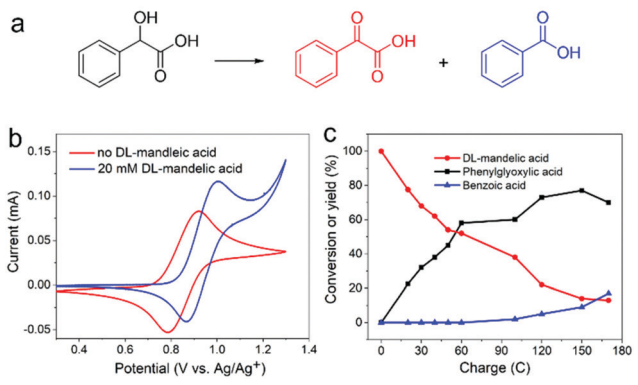

Fig. 2 (a) Oxidation of DL-mandelic acid can produce phenylglyoxylic acid and benzoic acid. (b) Cyclic voltammograms collected with 5 mM NHPI and 25 mM 2,6-lutidine in 0.1 M $LiClO_4$ MeCN/H_2O (v/v: 2/1) in the absence and presence of 20 mM DL-mandelic acid (scan rate: 50 mV s^{-1}). (c) Changes in the conversion of DL-mandelic acid and yields of phenylglyoxylic acid and benzoic acid during electrolysis at 0.85 V *vs.* Ag/Ag^+.

It has been reported that the redox potential of NHPI can be altered upon the addition of an organic base.[37] Hence, three different organic bases were evaluated, including Et_3N, pyridine, and 2,6-lutidine (Fig. S1a–c†). In the presence of 2,6-lutidine, the cyclic voltammogram (CV) of DL-mandelic acid oxidation showed the most cathodic shift of its onset potential and the highest increased current (Fig. S1d†). Therefore, 2,6-lutidine was employed as the organic base in all the subsequent electrochemical studies unless noted otherwise. The solvent system was also optimized by varying the ratio between MeCN and H_2O. The CVs of DL-mandelic acid oxidation in the presence of NHPI and 2,6-lutidine in each electrolyte were shown in Fig. S2.† Furthermore, electrolysis was conducted at 0.85 V *vs.* Ag/Ag^+. After passing the theoretical amount of charge (60 C), the highest yield of phenylglyoxylic acid could be obtained as 60% in 0.1 M $LiClO_4$ MeCN/H_2O (v/v: 2/1) (Table S1†). Therefore, 0.1 M $LiClO_4$ MeCN/H_2O (v/v: 2/1) was selected as the optimal electrolyte for all the electrochemical experiments. Finally, the ratio between 2,6-lutidine and NHPI was also optimized. Along the increasing ratio between 2,6-lutidine and NHPI from 0.5 to 6, a cathodic shift of its redox potential was observed in 0.1 M $LiClO_4$ MeCN/H_2O (v/v: 2/1), from 1.1 V to 0.85 V (*vs.* Ag/Ag^+) along with improved reversibility (Fig. S3†). Since the cyclic voltammograms collected with the 2,6-lutidine/NHPI ratio of 5 and 6 were nearly identical (Fig. S3†), all the following electrochemical experiments were conducted with five equivalents of 2,6-lutidine *versus* one equivalent of NHPI. The linear dependence of the peak current of NHPI oxidation on the square root of scan rate confirmed that the electrochemical oxidation of NHPI under our experimental condition is a diffusion-controlled and homogenous process (Fig. S4†). As shown in Fig. 2b, upon the addition of 20 mM DL-mandelic acid, an increased anodic current was observed together with an anodic shift. This suggests that oxidized NHPI promotes the oxidation of DL-mandelic acid and that DL-mandelic acid slightly neutralizes 2,6-lutidine. Such a conclusion is supported by the further anodic shift of the redox feature along with increasing concentration of DL-mandelic acid (Fig. S5†). When the concentration of DL-mandelic acid exceeded 300 mM, no cathodic current could be detected, implying that all the oxidized NHPI was utilized to oxidize the acid substrate. The mechanism of DL-mandelic acid oxidation was shown in Fig. S6,† where NHPI was first deprotonated by 2,6-lutidine to form PINO. Then, PINO mediated the abstraction of the α hydrogen atom of DL-mandelic acid to generate a radical intermediate that was further oxidized to form phenylglyoxylic acid.

Next, long-term electrolysis was conducted at 0.85 V *vs.* Ag/Ag^+ and the resulting products were characterized and quantified *via* high-performance liquid chromatography (HPLC). Calibration curves of commercially purchased DL-mandelic, phenylglyoxylic acid, and benzoic acid were collected prior to electrolysis (Fig. S7†). Fig. 2c presents the conversion of DL-mandelic acid as a function of passed charge during the electrolysis. The desirable phenylglyoxylic acid was produced instantaneously once the electrolysis started. The yield of 60%

was achieved after passing the theoretical amount of charge while the highest yield of 77% could be obtained if the electrolysis was continued till 150 C charge passed. The side product benzoic acid was also detected, however showing a much lower yield (<20%).

After establishing the success of partial oxidation of DL-mandelic acid to phenylglyoxylic acid, subsequently we explored the reductive amination of the intermediate keto acid to the desirable amino acid (Fig. 3a). Because of the simple condensation reaction between ketone and amine groups, the initial transformation can proceed smoothly at room temperature in a relatively short period of time.[38] As shown in Fig. S8,† an oxime intermediate was formed by stirring phenylglyoxylic acid with $NH_2OH{\cdot}HCl$ for 24 hours in 0.1 M $LiClO_4$ MeCN/H_2O (v/v: 2/1). Notably, the reaction solvent is compatible with the initial electrochemical oxidation and the subsequent reduction steps, hence it is possible to directly transport the reaction mixture to the cathodic chamber of a flow electrolyzer without tedious and expensive separation or purification of the oxime intermediate. In order to minimize the competing H_2 evolution reaction (HER), a Ti foil was employed as the cathode. As shown in Fig. 3b, the blank linear sweep voltammogram was collected in 0.1 M $LiClO_4$ MeCN/H_2O (v/v: 2/1) and the onset potential of HER on Ti was *ca.* −0.7 V *vs.* Ag/Ag^+. Upon the addition of the oxime intermediate (20 mM), an apparent anodic shift of the onset potenital to −0.5 V *vs.* Ag/Ag^+ was observed, accompanied with a rapid cathodic current rise. Long-term electrolysis was performed at −1.0 V *vs.* Ag/Ag^+. Fig. 3c shows a comparison of the current and passed charge during electrolysis with and without the oxime intermediate. In the absence of oxime, very small background current and hence negligible accumulated charge were obtained. However, in the presence of the oxime intermediate, the catalytic current decreased from 6 to 1 mA within the first 200 minutes due to the conversion of the oxime intermediate. The passed charge was roughly 45 C at the end of this electrolysis. Proton NMR was performed to quantify 2-phenylglycine with 1,3,5-trimethoxybenzene as the internal standard. As shown in Fig. S9,† the yield of 2-phenylglycine was 93%, with 100% conversion of the starting compound and 93% faradaic efficiency.

The above batch electrolysis results proved the feasibility of our method for converting α-hydroxyl acids to amino acids. With the aim of developing an electrochemical strategy suitable for practical application on a large scale, we sought to further explore the direct synthesis of amino acids from biomass-derived α-hydroxyl acids in a flow electrolyzer. Electrosynthesis using a flow cell provides several advantages over batch reactors, such as efficient mass transfer, uniform distribution of potential and current, high and stable production rate, and hence convenient scalability.[39]

Following the same strategy in batch electrolysis, DL-mandelic acid was also used to optimize the condition for flow electrolysis. Carbon paper and Ti foil were utilized as the anode and cathode, respectively, in a two-electrode configuration which were separated by an organic anion exchange membrane (Fumasep Fab-PK-130). The schematic diagram of flow electrolysis was illustrated in Fig. S10,† wherein α-hydroxyl acids were pumped into anodic chamber to form α-keto acids, which later reacted with an external nitrogen source (*e.g.*, NH_2OH or NH_3) and flowed back to the cathodic chamber. Reaction steps from DL-mandelic acid to 2-phenylglycine are presented in Fig. 4a. Firstly, DL-mandelic acid was oxidized to phenylglyoxylic acid, which reacted with $NH_2OH{\cdot}HCl$ to form an oxime intermediate. Subsequent electrochemical reduction resulted in 2-phenylglycine as the final product. As plotted in Fig. 4b, the linear sweep voltammogram of the flow cell without

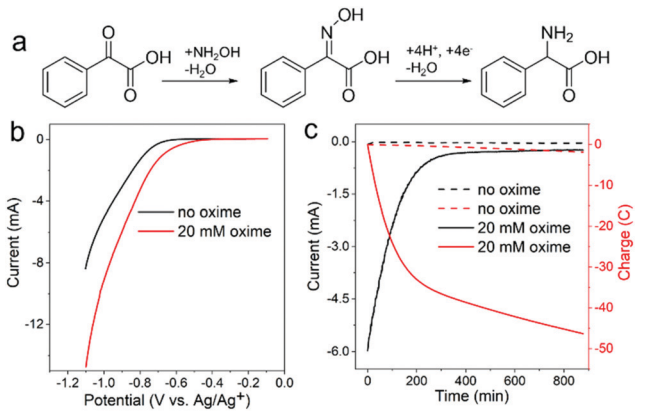

Fig. 3 (a) Reductive amination of phenylglyoxylic acid to yield 2-phenylglycine. (b) Linear sweep voltammograms collected on a Ti cathode in 0.1 M $LiClO_4$ MeCN/H_2O (v/v: 2/1) in the absence or presence of the oxime intermediate (scan rate: 50 mV s^{-1}). (c) Changes in current and accumulated charge during electrolysis at −1.0 V *vs.* Ag/Ag^+ in 0.1 M $LiClO_4$ MeCN/H_2O (v/v: 2/1) with and without 20 mM oxime.

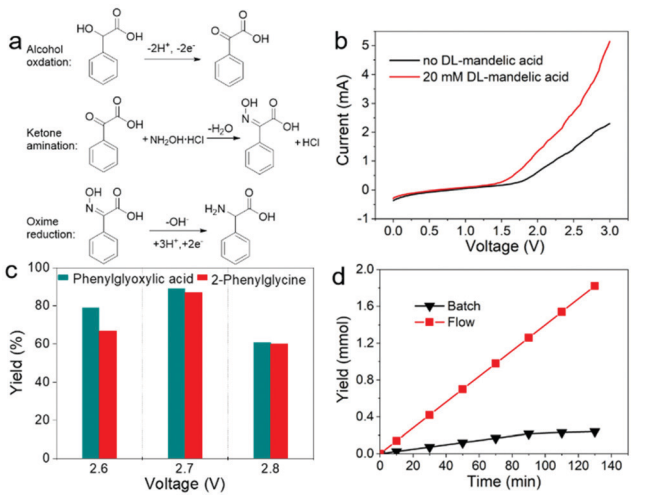

Fig. 4 (a) Reaction steps for the electrosynthesis of 2-phenylglycine from DL-mandelic acid. (b) Linear sweep voltammograms of a two-compartment flow cell with and without 20 mM DL-mandelic acid in 0.1 M $LiClO_4$ MeCN/H_2O (v/v: 2/1) with 5 mM NHPI and 25 mM 2,6-lutidine. (c) Comparison of the yields of phenylglyoxylic acid and 2-phenylglycine obtained at different applied voltages in a flow cell. (d) Yield change of phenylglyoxylic acid during electrolysis using either a batch electrolyzer or a flow electrolyzer.

DL-mandelic acid shows an onset voltage for water splitting at *ca.* 1.8 V. Once 20 mM DL-mandelic acid was added into the anode electrolyte, a rising current was observed beyond 1.5 V. Three electrolysis experiments were conducted with applied voltage of 2.6, 2.7, and 2.8 V. As expected, phenylglyoxylic acid and 2-phenylglycine were detected in the anode and cathode outlets, respectively (Fig. S11†). The yields of these two compounds were compared in Fig. 4c. It is apparent that the applied voltage of 2.7 V resulted in the highest yields for both phenylglyoxylic acid (89%) and 2-phenylglycine (87%). Notably, the yield of phenylglyoxylic acid was 89%, which was higher than that obtained from batch electrolysis (77%). By analysing the yield of phenylglyoxylic acid over time and comparing it with the yields obtained from batch electrolysis (Fig. 4d), it is clear that flow electrolysis exhibits linear increase in the production of the desirable product as opposed to batch electrolysis which is limited by the starting concentration of the substrate. In the case of batch electrolysis, the reaction rate decreases dramatically when the starting material is being consumed.

The realization of electrochemical synthesis of 2-phenylglycine from DL-mandelic acid in a flow electrolyzer prompted us to expand the scope of biomass-derived α-hydroxyl acids for the synthesis of natural amino acids. As shown in Fig. 5, following the same electrochemical condition described above, another aromatic α-hydroxy acid, DL-3-phenyllactic acid, could also be transformed to yield phenylpyruvic acid with a high yield of 92% (Fig. S12 and S13†), and the subsequent reductive amination using NH_3 (aq.) as the nitrogen source resulted in the natural amino acid phenylalanine (Phe) with a desirable yield of 100% (Fig. S14†). Furthermore, aliphatic hydroxyl acids can also be equally converted to their corresponding natural amino acids in a similar fashion. For instance, three representative aliphatic hydroxyl acids, 2-hydroxyacetic acid, 2-hydroxypropanoic acid, and 2-hydroxy-4-methylpentanoic acid were explored, and their intermediate keto acids were produced with yields around 70% (Fig. S15–S17†). Subsequent reductive amination led to glycine (Gly), alanine (Ala), and leucine (Leu) with yields of 70%, 80%, and 100%, respectively (Fig. S18–S20†), superior to reported photocatalytic strategies.

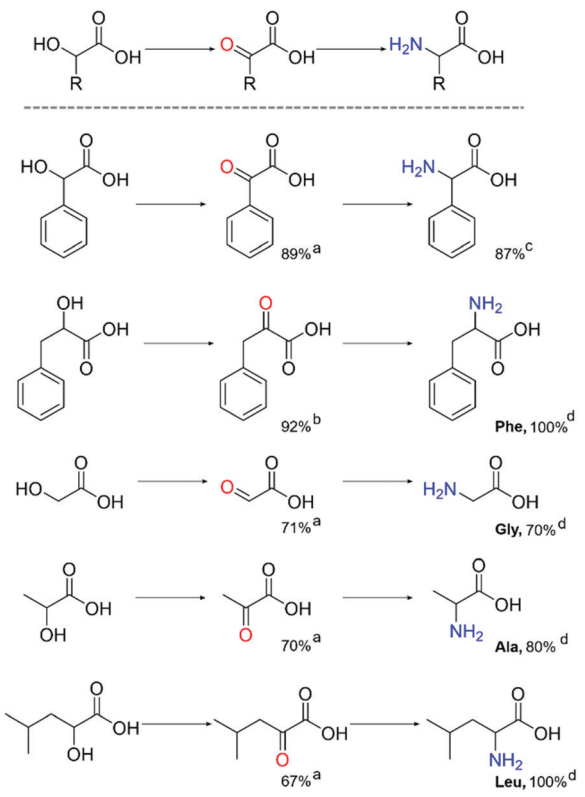

Fig. 5 Substrate scope on electrosynthesis of amino acids with a flow cell at 2.7 V in 0.1 M $LiClO_4$ MeCN/H_2O (v/v: 2/1). Reaction condition: 5 mM mediator, 25 mM 2,6-lutidine and 20 mM substrates in each chamber with a flow rate of 0.8 mL min^{-1}. [a]NHPI as mediator, [b]TEMPO as mediator, [c]$NH_2OH{\cdot}HCl$ as the nitrogen source, and [d]NH_3 (aq.) as the nitrogen source.

Conclusion

In summary, we have reported an electrochemical strategy for the direct synthesis of amino acids, including four natural amino acids (Phe, Gly, Ala, and Leu), from biomass-derived and inexpensive α-hydroxyl acids under ambient conditions (*e.g.*, room temperature and atmospheric pressure). Low-cost ammonium hydroxide or ammonia was utilized as the nitrogen source. Our electrochemical approach consists of two steps: selective oxidation of α-hydroxyl acids at the anode and reductive amination of the oxime (or imine) intermediates at the cathode using the same electrolyte. Such a strategy takes advantages of both oxidation and reduction reactions in one flow cell. Overall, this electrochemical synthetic strategy represents a greener approach for the production of amino acids using sustainable carbon source as the starting materials, which is also attractive for large-scale application.

Conflicts of interest

There are no conflicts to declare.

Acknowledgements

Y. S. acknowledges the financial support of the National Science Foundation (CHE-2102220), the Herman Frasch Foundation (820-HF17), and the University of Cincinnati. NMR experiments were performed on a Bruker AVANCE NEO 400 MHz NMR spectrometer (funded by NSF-MRI grant CHE-1726092).

References

1 H. Luo, E. P. Weeda, M. Alherech, C. W. Anson, S. D. Karlen, Y. Cui, C. E. Foster and S. S. Stahl, *J. Am. Chem. Soc.*, 2021, **143**, 15462–15470.

2 U. Nwosu, A. Wang, B. Palma, H. Zhao, M. A. Khan, M. Kibria and J. Hu, *Renewable Sustainable Energy Rev.*, 2021, **148**, 111266.
3 B. You, X. Liu, N. Jiang and Y. Sun, *J. Am. Chem. Soc.*, 2016, **138**, 13639–13646.
4 B. You, N. Jiang, X. Liu and Y. Sun, *Angew. Chem., Int. Ed.*, 2016, **55**, 9913–9917.
5 S. Song, V. Fung Kin Yuen, L. Di, Q. Sun, K. Zhou and N. Yan, *Angew. Chem., Int. Ed.*, 2020, **59**, 19846–19850.
6 Y. Wang, S. Furukawa, S. Song, Q. He, H. Asakura and N. Yan, *Angew. Chem.*, 2020, **132**, 2309–2313.
7 H. Wu, H. Li and Z. Fang, *Green Chem.*, 2021, **23**, 6675–6697.
8 T. Hermann, *J. Biotechnol.*, 2003, **104**, 155–172.
9 G. Wu, *Amino Acids*, 2013, **45**, 407–411.
10 G. Wu, *Adv. Nutr.*, 2010, **1**, 31–37.
11 Y. Izumi, I. Chibata and T. Itoh, *Angew. Chem., Int. Ed. Engl.*, 1978, **17**, 176–183.
12 S. J. Zuend, M. P. Coughlin, M. P. Lalonde and E. N. Jacobsen, *Nature*, 2009, **461**, 968–970.
13 H. Yan, J. Suk Oh, J.-W. Lee and C. E. Song, *Nat. Commun.*, 2012, **3**, 1212.
14 N. Yan and Y. Wang, *Chem*, 2019, **5**, 739–741.
15 M. D'Este, M. Alvarado-Morales and I. Angelidaki, *Biotechnol. Adv.*, 2018, **36**, 14–25.
16 W. Deng, Y. Wang, S. Zhang, K. M. Gupta, M. J. Hülsey, H. Asakura, L. M. Liu, Y. Han, E. M. Karp, G. T. Beckham, P. J. Dyson, J. W. Jiang, T. Tanaka, Y. Wang and N. Yan, *Proc. Natl. Acad. Sci. U. S. A.*, 2018, **115**, 5093–5098.
17 S. Song, J. Qu, P. Han, M. J. Hülsey, G. Zhang, Y. Wang, S. Wang, D. Chen, J. Lu and N. Yan, *Nat. Commun.*, 2020, **11**, 4899.
18 Z. Wan, D. Wang, Z. Yang, H. Zhang, S. Wang and A. Lei, *Green Chem.*, 2020, **22**, 3742–3747.
19 F. Ling, T. Liu, C. Xu, J. He, W. Zhang, C. Ling, L. Liu and W. Zhong, *Green Chem.*, 2022, **24**, 1342–1349.
20 F. Ling, D. Cheng, T. Liu, L. Liu, Y. Li, J. Li and W. Zhong, *Green Chem.*, 2021, **23**, 4107–4113.
21 T. Fukushima and M. Yamauchi, *Chem. Commun.*, 2019, **55**, 14721–14724.
22 M. S. Holm, S. Saravanamurugan and E. Taarning, *Science*, 2010, **328**, 602–605.
23 F. F. Wang, C. L. Liu and W. S. Dong, *Green Chem.*, 2013, **15**, 2091–2095.
24 L. Li, F. Shen, R. L. Smith and X. Qi, *Green Chem.*, 2017, **19**, 76–81.
25 S. Zheng, J. Yan and K. Wang, *Eng. J.*, 2021, **7**, 22–32.
26 T. Noël, Y. Cao and G. Laudadio, *Acc. Chem. Res.*, 2019, **52**, 2858–2869.
27 M. Atobe, H. Tateno and Y. Matsumura, *Chem. Rev.*, 2018, **118**, 4541–4572.
28 M. A. Abdel Rahim, H. B. Hassan and R. M. Abdel Hamid, *J. Power Sources*, 2006, **154**, 59–65.
29 M. Asgari, M. G. Maragheh, R. Davarkhah, E. Lohrasbi and A. N. Golikand, *Electrochim. Acta*, 2012, **59**, 284–289.
30 C. H. Lam, A. J. Bloomfield and P. T. Anastas, *Green Chem.*, 2017, **19**, 1958–1968.
31 P. N. Amaniampong, Q. T. Trinh, J. J. Varghese, R. Behling, S. Valange, S. H. Mushrif and F. Jérôme, *Green Chem.*, 2018, **20**, 2730–2741.
32 K. Gorgy, J. C. Lepretre, E. Saint-Aman, C. Einhorn, J. Einhorn, C. Marcadal and J. L. Pierre, *Electrochim. Acta*, 1998, **44**, 385–393.
33 J. E. Nutting, M. Rafiee and S. S. Stahl, *Chem. Rev.*, 2018, **118**, 4834–4885.
34 M. Rafiee, B. Karimi and S. Alizadeh, *ChemElectroChem*, 2014, **1**, 455–462.
35 M. Masui, T. Ueshima and S. Ozaki, *J. Chem. Soc., Chem. Commun.*, 1983, **8**, 479–480.
36 M. Ohara, C. Y. Chen and T. Kwan, *Bull. Chem. Soc. Jpn.*, 1966, **39**, 137–140.
37 I. Bosque, G. Magallanes, M. Rigoulet, M. D. Kärkäs and C. R. Stephenson, *ACS Cent. Sci.*, 2017, **3**, 621–628.
38 T. Fukushim and M. Yamauchi, *J. Appl. Electrochem.*, 2021, **51**, 99–106.
39 M. Atobe, *Curr. Opin. Electrochem.*, 2017, **2**, 1–6.